

# Antineuroinflammatory effects of dl-3-n-butylphthalide conferred by stimulation of Foxp3 and Ki-67 in an ischemic stroke model

**Xi Liu**

Peking University Health Science Centre

**Runzhe Liu**

Peking University Health Science Centre

**Dongxu Fu**

Institute of High Energy Physics Chinese Academy of Sciences

**Hao Wu**

Peking University Health Science Centre

**Xin Zhao**

Peking University Health Science Centre

**Yi Sun**

Peking University Health Science Centre

**Meng Wang**

Institute of High Energy Physics Chinese Academy of Sciences

**Xiaoping Pu** (✉ [pxp123@bjmu.edu.cn](mailto:pxp123@bjmu.edu.cn))

Peking University

---

## Research

**Keywords:** dl-3-n-butylphthalide, ischemia, neuroinflammation, MALDI-TOF-MSI, LA-ICP-MSI

**Posted Date:** April 24th, 2020

**DOI:** <https://doi.org/10.21203/rs.3.rs-22724/v1>

**License:** © ⓘ This work is licensed under a Creative Commons Attribution 4.0 International License.

[Read Full License](#)

---

# Abstract

## Background

DI-3-n-butylphthalide (NBP) has been widely used for the treatment of ischemic stroke in China. However, its mechanisms of action have not been fully elucidated.

## Methods

We established a permanent middle cerebral artery occlusion (pMCAO) rat model and administered 4 mg/kg/d NBP by tail vein injection for 9 days. Changes in some molecules related to neuroinflammation, neovascularization and nerve regeneration were observed, such as MALDI-TOF MSI to study the distribution of phospholipids in the brain, LA-ICP MSI to observe the changes of Foxp3, Ki-67 and pCREB, immunohistochemistry to investigate NLRP3 and its downstream inflammatory products Caspase-1 and IL-1 $\beta$ .

## Results

These results showed that NBP attenuated ischemic damage in pMCAO rats, accompanied by improving neurological deficits. It was revealed for the first time in an animal stroke model that NBP decreased the levels of PE (18:0), NLRP3, Caspase-1 and IL-1 $\beta$ , while increasing the levels of several phospholipids, such as PA (16:0/18:1), PA (18:0/22:6), PE (16:0/22:6), PE (P-18:0/22:6), PE (18:0/22:6), PS (18:0/22:6), PI (18:0/20:4), Foxp3, Ki-67 and pCREB, in the ischemic brain region.

## Conclusion

These results provide evidence that NBP can reduce neuroinflammation in brain tissue and promote the regeneration of nerves and blood vessels, thus exerting a protective effect on neuromorphology and function.

## Introduction

With over two million new cases annually, stroke is associated with the most disability-adjusted life-years lost of any disease in China.<sup>1</sup> Ischemic stroke is mainly caused by the occlusion of cerebrovascular vessels, which leads to insufficient blood oxygen supply and necrosis of brain tissue.

Inflammation plays an important role in the overall pathogenesis of ischemic stroke. Studies in animal models have revealed that innate and adaptive immune responses occur minutes to weeks or even months after ischemic stroke injury.<sup>2</sup> Cerebral ischemia can trigger inflammatory responses, including the activation of microglia, macrophages, neutrophils, and dendritic cells.<sup>3</sup> Proinflammatory factors are

released, leading to the death of brain neurons and glial cells.<sup>4</sup> Furthermore, stroke has systemic effects that result in a spike in inflammatory cytokines during the initial activation phase, which is followed by severe immunosuppression linked to atrophy of the spleen and thymus in MCAO-induced stroke models in mice.<sup>5</sup> However, inflammatory cytokines that have negative impacts on recovery and are associated with increased damage volume, including IL-1 $\beta$ , E-selectin, and vascular adhesion molecules, are more commonly studied.<sup>6</sup>

DI-3-n-butylphthalide (NBP) was first discovered in the seeds of *Apium graveolens Linn* and was approved by the National Medical Products Administration (NMPA) in 2002 as an anti-ischemic stroke drug.<sup>7</sup> A number of studies have shown that NBP can improve post-stroke symptoms through various mechanisms, including inflammation, collateral circulation, mitochondrial function, apoptosis, and oxidative stress.<sup>8</sup> NBP ameliorates experimental autoimmune encephalomyelitis by suppressing PGAM5-induced necroptosis and inflammation in microglia.<sup>2</sup> NBP improves lipopolysaccharide-induced depressive-like behavior in rats through the involvement of the Nrf2 and NF- $\kappa$ B pathways.<sup>9</sup> Geng et al. investigated metabolite biomarkers associated with NBP in hippocampal tissue in a lipopolysaccharide (LPS)-induced rat model of depression. Most of the identified differentially expressed metabolites were related to amino acids, lipids, energy, and oxidative stress metabolism. The findings provide insight into the anti-inflammatory effects of NBP.<sup>10</sup> However, few studies have reported the mechanisms of the effects of NBP in in situ animal stroke models. In a previous study, we used matrix-assisted laser desorption ionization time-of-flight mass spectrometry imaging (MALDI-TOF MSI) to evaluate the effect of NBP on changes in small molecules in the brains of pMCAO model rats and discovered that NBP can alleviate the abnormal accumulation of glucose and citric acid in the brains of pMCAO model rats, enhance ATP metabolism, and improve the glutamate-glutamine cycle in the brain. It can also increase the content of antioxidants and the balance of metal ions.<sup>11</sup>

Regulatory T ( $T_{reg}$ ) cells play an important role after stroke and have become a research hotspot in the field of immune diseases.  $T_{reg}$  cells maintain immune tolerance and play a key role in tissue homeostasis and remodeling.<sup>12</sup> The development and function of  $T_{reg}$  cells is closely related to the expression of its specific transcription factor Foxp3.<sup>13,14</sup> And a lack of Foxp3 can lead to the loss of  $T_{reg}$  cell function.<sup>15</sup> However, no studies have reported the effect of NBP on  $T_{reg}$  cells or Foxp3.

Stubbe T et al reported that approximately 60% of Foxp3(+) Tregs in the ischemic hemisphere are positive for the proliferation marker Ki-67 on days 7 and 14 after MCAO. The transfer of naive CD4(+) cells lacking Foxp3(+) Tregs into RAG1(-/-) mice 1 day before MCAO does not lead to the de novo generation of Tregs 14 days after surgery. After the depletion of CD25(+) Tregs, no changes in neurological outcome are detected. The sustained presence of Tregs in the brain after MCAO indicates a long-lasting immunological alteration and involvement of brain cells in immunoregulatory mechanisms.<sup>16</sup>

This study aimed to provide further evidence of NBP's effects of anti-inflammation, regeneration of nerves and blood vessels. We utilized MALDI-TOF MSI, laser ablation-inductively coupled plasma mass

spectrometry imaging (LA-ICP MSI) and immunochemistry. The effects of NBP on several molecules, including phospholipids (potential biomarkers of inflammation), NLRP3, Caspase-1, IL-1 $\beta$ , Foxp3 (a Treg marker), Ki-67 and pCREB, in the ipsilateral hemispheres of the brains of animal stroke models were studied for the first time.

## Material And Methods

### Material

Healthy male 8- to 10-week-old SD rats weighing 280–310 g were purchased from Beijing Vital River Experimental Animal Technology Co., Ltd. (license number: SCXK (Beijing) 2012-0001). The rats were housed in an SPF-level laboratory at the Experimental Animal Department of Peking University Health Science Center. The rats were kept under standard environmental conditions ( $23 \pm 1$  °C, humidity  $45\% \pm 5\%$ , 12-h light/dark cycle) and had free access to standard food (Keaoxieli, Beijing, China) and drinking water.

Injectable NBP (Fig. 1A) was provided by China Shijiazhuang Pharmaceutical Company Co., Ltd. (batch number: 17051026). Edaravone was obtained from Simcere Pharmaceutical Co., Ltd. (batch number: 80-181203). Injectable urinary kallidinogenase (UK) was purchased from Guangdong Tianpu Biochemical Pharmaceutical Co., Ltd. and served as the positive control drug (batch number: 311701021).

The antibodies used in this study are listed in Table 1.

Table 1  
Antibodies used in this study.

Antibodies	Source	Identifier
Cell-ID™ Intercalator-Ir	Fluidigm	Cat# 201192A
Anti-Mouse/Rat Foxp3 (FJK-16 s)-165Ho	Fluidigm	Cat# 3165024A
Anti-Ki-67(B56)-168Er	Fluidigm	Cat# 3168022D
Anti-pCREB[S133](87G3)-176Yb	Fluidigm	Cat# 3176005A
Anti-NLRP3	Abcam	Cat# ab214185
Anti-IL-1 $\beta$	Abcam	Cat# ab9722
Anti-Caspase-1	Immunoway	Cat# YT5743

### Model establishment and drug administration

The establishment of the rat pMCAO model was in accordance with our previous study.<sup>11</sup> Rats were anesthetized by an intraperitoneal injection of 0.35 g/kg chloral hydrate. The right common carotid artery and the external carotid artery were exposed after an incision was made in the neck. Then, the right

external carotid artery and the proximal end of the common carotid artery were ligated with a suture. A "V"-shaped cut was made at the distal end of the common carotid artery, and a thread was inserted through the incision to the internal carotid artery. When the thread was inserted 15–16 mm into the internal carotid artery and the resistance increased significantly, insertion was stopped, and the thread was tied to the distal end of the common carotid artery with a suture to fix it. The incision in the neck was then sutured and disinfected with medical-grade alcohol. The surgery was completed within 15 min, and the rats woke after approximately 2 h. Only the rats that rotated to the left were considered successful models. The sham surgery group underwent a similar operation, but the common carotid artery was left intact, and a thread was not inserted.

After surgery, approximately 60% rats developed stroke symptoms and were considered successful models. These animals were randomly divided into 5 groups of 15 rats each: the model group, the NBP-treated group, the edaravone (ED, positive control drug)-treated group and the urinary kallidinogenase (UK, positive control drug)-treated group. Drug administration was started 2 h after the end of modeling. In the NBP group, 4 mg/kg NBP injection (q.d.) was administered through the tail vein;<sup>11</sup> in the ED group, 5 mg/kg edaravone (q.d.) was administered through the tail vein; and in the UK group, 0.013 PNA/kg UK (q.d.) was administered via the tail vein. The sham surgery group and model group were given the same volume of normal saline (q.d.). The drugs were administered for 9 days.

At the end of drug administration, 6 rats were randomly selected from each group for the following study (Fig. 1B).

## Behavioral test

The modified neurological severity score (mNSS) test was used to evaluate the degree of neurological deficit after the establishment of the rat pMCAO model. It included exercise, sensory, reflex and balance tests. In this study, the mNSS score was determined according to the method described by Chen.<sup>17</sup> A higher mNSS score indicated more severe neurobehavioral damage.

## MALDI-TOF MSI for the detection of small molecules in brain tissue

Three rats from each group were perfused with normal saline, and the brains were quickly collected, frozen in liquid nitrogen, and stored at -80 °C before slicing. Frozen brain tissues were sliced into 10- $\mu$ m thick sections beginning at 0.6 mm from bregma and then mounted on the indium-tin oxide coated surface of a glass slide for MALDI-TOF MSI. MALDI-TOF MSI was conducted and analyzed according to the method described by Liu Huihui.<sup>18</sup> An ultrafleXtreme MALDI-TOF/TOF MS (Bruker Daltonics, Billerica, USA) equipped with a Smartbeam Nd: YAG 355 nm laser was utilized for MALDI analysis. Negative-ion mass spectra were acquired in reflector mode with a pulsed ion extraction time of 80 ns, an accelerating voltage of 20.00 kV, an extraction voltage of 17.90 kV, a lens voltage of 5.85 kV, and a reflector voltage of 21.15 kV. For MSI analysis, the imaging spatial resolution of brain tissues from rats was set to 100  $\mu$ m.

The regions of interest were manually defined in the imaging software using both the optical image and MSI data image.

## Histopathological observation

The other 3 rats from each group were perfused with normal saline and formalin and fixed in formalin overnight. Four-micrometer-thick paraffin slices 0.6 mm from bregma were prepared for HE staining. Pathological changes in the brain were observed under Motic Tele-Microscope System (Motic China Group, Xiamen, China).

## LA-ICP MSI for the observation of Foxp3, Ki-67 and pCREB distribution in brain tissue

FFPE (formalin-fixed and paraffin-embedded) brain tissues were sectioned at a thickness of 4  $\mu\text{m}$  for LA-ICP MSI.<sup>19</sup> Staining for anti-Foxp3 (FJK-16 s)-165Ho, anti-Ki-67 (B56)-168Er, and anti-pCREB [S133] (87G3)-176Yb was performed manually. The tissue sections were baked for 2 h at 60 °C in a slide oven. Then, the tissue sections were dewaxed in fresh xylene for 20 min and rehydrated in a graded series of alcohols (absolute ethanol, and 95:5, 80:20, 70:30, and 0:100 ethanol:deionized water; 5 min each). Heat-induced epitope retrieval was conducted in Tris-EDTA buffer, pH 9, in a 96 °C water bath for 30 min. After immediate cooling, the sections were washed with deionized water and PBS for 10 min each and then blocked with 3% BSA in PBS for 45 min. The sections were incubated overnight at 4 °C with an antibody master mix (anti-Foxp3 (FJK-16 s)-165Ho: 1:50 dilution; anti-Ki-67 (B56)-168Er: 3:100 dilution; anti-pCREB [S133] (87G3)-176Yb: 1:100 dilution). After 2 8-min washes in 0.2% Triton X-100 in PBS and 2 8-min washes in PBS, the sections were incubated with Cell-ID™ Intercalator-Ir (125  $\mu\text{M}$ ) in PBS (1:400 dilution) for 30 min at room temperature. After being washed, the sections were dried at room temperature before LA-ICP MSI.

An NWR 213 laser ablation system (Elemental Scientific Lasers, Bozeman, USA) coupled to a NexION 300D ICP-MS (Perkin Elmer, Waltham, USA) was utilized for LA-ICP MSI analysis. Helium was utilized as the ablation gas and introduced with argon gas through a T-piece into the ICP-MS after the ablation cell. The LA-ICP-MS was calibrated with NIST 612 glass standards for high U signal intensity while keeping the oxide production (i.e.,  $\text{UO}^+/\text{U}^+$  ratio) at a low level. The LA-ICP-MS operating parameters are shown in Table 2. The laser ablation parameters, including spot size, laser energy, scan rate, and ablation frequency, were carefully chosen to guarantee quantitative ablation of the brain sections and minimal ablation of the glass slides. All brain sections were ablated using a line ablation mode, where ICP-MS was triggered by a laser shot, and the data were acquired by ICP-MS in the time-resolved analysis mode. The acquired data were processed into images by lolite software (V3.6, serial number: 74272) .<sup>20</sup>

Table 2  
Operating parameters of LA-ICP-MS for elemental imaging

ICP-MS		Laser ablation	
Nebulizer gas	0.94 L min <sup>-1</sup>	He carrier gas	0.60 L min <sup>-1</sup>
Auxiliary gas	0.50 L min <sup>-1</sup>	Ablation frequency	20 Hz
Plasma gas	18.0 L min <sup>-1</sup>	Spot size	100 μm
RF power	1300 W	Scan speed	100 μm s <sup>-1</sup>
Acquisition mode	Time-resolved analysis	Fluence	2.05 J cm <sup>-2</sup>
Isotope monitored	<sup>165</sup> Ho, <sup>168</sup> Er, <sup>176</sup> Yb, <sup>193</sup> Ir		
Dwell time	50 ms per isotope		

## Immunohistochemistry

For immunohistochemistry, FFPE brain tissue sections were stained with prediluted antibodies, including anti-NLRP3 (1:100 dilution), anti-Caspase-1 (1:50 dilution), and anti-IL-1β (1:100 dilution), according to standard protocols.<sup>21</sup> Briefly, the sections were baked, dewaxed, and rehydrated as described above. Heat-induced epitope retrieval was conducted in sodium citrate, pH 6, in a 96 °C water bath for 30 min. After immediate cooling, the sections were washed with deionized water and PBS for 5 min each. The slides were incubated with 3% H<sub>2</sub>O<sub>2</sub> in PBS for 1 h at 37 °C and then washed 3 × 5 min with PBS. The sections were blocked with 10% normal serum/0.3% Triton X-100 in PBS for 1 h at 37 °C. The sections were incubated overnight at 4 °C with primary antibody (diluted in PBS/1% BSA). The samples were then washed 3 × 5 min with PBS. The sections were incubated with HRP-conjugated goat anti-rabbit IgG H&L as the secondary antibody for 1 h at 37 °C. After further washing three additional 5-min washes with PBS, immunoperoxidase staining was developed using a 3,3'-diaminobenzidine (DAB) chromogen (Dako) for 5 min. The slides were washed with deionized water for 5 min, dehydrated in graded alcohol and xylene, mounted and coverslipped. Changes in the brain were observed under an optical microscope (Motic Tele-Microscope System, Motic China Group Co., Ltd.).

## Statistical analysis

Statistical analysis was performed using GraphPad Prism software. The data are expressed as the mean ± standard deviation (mean ± SD). The distribution of data was tested with Shapiro-Wilk normality test. One-way ANOVA was used for comparisons between groups, and  $P < 0.05$  was considered statistically significant.

## Results

# **NBP improves the neurobehavioral performance and cerebral damage in the pMCAO rat model**

As shown in Fig. 1C, compared with that of the sham surgery group, the mNSS of the model group increased after 9 days ( $P < 0.001$ ), indicating severe neurobehavioral damage. The NBP group exhibited a lower mNSS than the model group ( $P < 0.05$ ). The mNSS of the edaravone-treated group and the UK-treated group decreased less than the mNSS of the NBP group.

As shown in Fig. 1D, compared with that of the sham surgery group, the survival rate of the model group decreased after 9 days ( $P < 0.001$ ), and the survival rates of the NBP, UK and edaravone groups were lower than the survival rate of the sham surgery group but higher than that of the pMCAO group.

HE staining of FFPE sections of brain tissue (Fig. 1E) showed that the striatal area of the sham surgery group had normal morphology, neat arrangement, rich cytoplasm and central nuclei. The model group had a large area of cell lysis, a large vacuolar area, a loose interstitium, broken cell structure, nuclear pyknosis and deep staining. The NBP group and UK groups showed improvement compared with the model group, exhibiting less cell lysis and a lower degree of interstitial loosening. The lesion area in brain tissues from each group was computed, and the lesion area in the model group was significantly increased compared with that in the sham surgery group ( $P < 0.001$ ). The areas of brain tissue damage in the NBP group and the positive control UK group were significantly decreased (both  $P < 0.05$ ) compared with that of the model group.

## **NBP affects the distribution of phospholipid molecules in the brain tissues of ischemic rats**

MALDI-TOF MSI showed (Fig. S1) that on the ischemic side of the brain, NBP alleviated the abnormal accumulation of glucose and citric acid, enhanced ATP metabolism, improved the glutamate-glutamine cycle, and increased the content of antioxidants. These results are consistent with our previous study<sup>11</sup>.

Furthermore, we also found (Fig. 2A) that the distribution of phospholipid PE (18:0) in the in the right cortex and striatum of the model group was increased compared with that in the sham surgery group, while the NBP group had a reduced distribution of phospholipid PE (18:0) in these areas. PA (16:0/18:1), PA (18:0/22:6), PE (16:0/22:6), PE (P-18:0/22:6), PE (18:0/22:6), PS (18:0/22:6), and PI (18:0/20:4) were decreased in the right cortex and striatum of the model group compared with the sham surgery group, while the NBP group had increased levels of these molecules. There were obvious differences in the average mass spectrometry signal intensities between the pMCAO and NBP-treated groups in the ischemic areas (Fig. 2B, C), which was consistent with the imaging results.

## **NBP changes the distribution of Foxp3, Ki-67 and pCREB in the brain tissues of pMCAO rats**

The intercalator  $^{193}\text{Ir}$  is a dye that specifically binds to the nucleus. The results of LA-ICP MSI (Fig. 3) revealed decreased  $^{193}\text{Ir}$  signals in the right cortex and striatum of the model group compared with the sham surgery group. The administration of NBP increased the distribution of  $^{193}\text{Ir}$  in these areas. These results indicated that NBP reduced cell death in the cortical and striatal regions of the brains of ischemic animals. The administration of the positive control drug UK had similar effects as those of NBP.

The levels of Foxp3, Ki-67, and pCREB in the in the right cortex and striatum of the model group were reduced compared with those in the sham group, and the administration of NBP increased the levels of Foxp3, Ki-67, and pCREB. The administration of the positive control drug UK had similar effects as those of NBP.

## Immunohistochemistry

Immunohistochemistry was used to detect the production of NLRP3 and its downstream inflammatory products Caspase-1 and IL-1 $\beta$  in the rat central nervous system. The results showed (Fig. 4) that compared with that in the sham surgery group, the expression of NLRP3 and Caspase-1 was increased in the right striatum of the model group and that the distribution of IL-1 $\beta$  was abnormal. NBP improved the abnormal expression of NLRP3 and Caspase-1 in the right striatum and the abnormal distribution of IL-1 $\beta$  in the model rats compared with the model rats, and the UK group also showed similar improvements.

## Discussion

Middle cerebral artery occlusion is a common model for ischemic stroke. In this study, the modified Longa method,<sup>22</sup> which allows stable and reproducible modeling, is simple and can simulate clinical stroke caused by ischemia well, was used to prepare a permanent middle cerebral artery occlusion (pMCAO) model.

The modified neurological severity score test is a commonly used and preferred method for assessing the extent of neurological impairment in permanent and transient middle cerebral artery occlusion models. In this experiment, pMCAO rats showed obvious symptoms of neurological damage, while NBP improved the degree of neurological damage in pMCAO rats to some extent. Taken together with the pathological staining results in brain tissues, these data show that NBP can significantly reduce the area of brain damage area in this model, which is consistent with the existing research results.<sup>23</sup>

LA-ICP MSI is a new method of mass spectrometry imaging. Several metal-labeled antibodies bind specific proteins on a tissue slice, and then the tissue is ablated by a laser to produce aerosol, which is transported by a carrier gas into plasma to complete ionization. Then, the ions are detected by mass spectrometry, and a distribution map of various proteins in a single test is obtained. LA-ICP MSI is simple, fast, high-throughput, and highly accurate and has a low operating cost, and it is gradually becoming a widely used imaging method.<sup>24</sup>

The mechanisms of brain damage in ischemia mainly involve the consumption of oxygen and energy (within a few minutes), the release of excitatory amino acids (within a few hours), the inflammatory response and apoptosis. These biochemical reactions mediate the death of nerve cells. Accordingly, one of the important early treatment methods for cerebral infarction is preventing the biochemical reactions of these processes, thereby blocking the death of nerve cells in brain tissue after cerebral vascular occlusion.

Phospholipids are important components of cell membranes and can indicate apoptosis, necrosis and the occurrence of excessive inflammation in cerebral ischemia. We used MALDI-TOF MSI technology to detect the distribution of phospholipid molecules in the brains of pMCAO rat models, which was very important for our study of the effect of NBP on the brain.<sup>25</sup> We found that PA (16:0/18:1), PA (18:0/22:6), PE (16:0/22:6), PE (P-18:0/22:6), PE (18:0/22:6), PS (18:0/22:6), PI (18:0/20:4) and other phospholipids were decreased in the ischemic area (right cortex and striatum), indicating that cell death occurred in ischemic cells; however, NBP alleviated cell death in ischemic cells. It is noteworthy that phospholipid PE (18:0) is abnormally increased in the ischemic area of the pMCAO model and that it is susceptible to oxidative stress for the formation of oxidized phospholipids. Oxidized phospholipids have a strong proinflammatory effect, indicating that NBP may inhibit the inflammatory reaction by indirectly affecting the excessive production of oxidized phospholipids.

The neuroinflammatory response promotes damage in cerebral ischemia. After cerebral ischemia, there is a severe inflammatory reaction in the brain tissue. In addition to inducing cell pyroptosis, excessive inflammatory factors promote apoptosis and necrosis.<sup>26</sup> The NLRP3 inflammasome in neurons and glial cells may play an important role in detecting cell damage and mediating inflammatory responses.<sup>27, 28</sup> During the innate immune response, the NLRP3 inflammasome regulates the activation of Caspase-1, which promotes the maturation of the cytokine pro-IL-1 $\beta$ . Additionally, the NLRP3 inflammasome regulates Caspase-1-dependent pyroptosis and induces cell death under pathological conditions of inflammation and stress.<sup>29</sup> Immunohistochemistry showed that NBP reduced the levels of NLRP3, IL-1 $\beta$  and Caspase-1 in the ischemic brain area, indicating that NBP can inhibit the inflammatory response mediated by the NLRP3 pathway. Similarly, Yang et al. suggested that NBP reduces neurovascular inflammation and ischemic brain injury in mice. This effect is associated with reduced infiltration of myeloid cells into the brain and improved cerebral blood flow after reperfusion.<sup>30</sup>

Regulatory T (T<sub>reg</sub>) cells are a special subset of T cells that are essential for inducing and maintaining the stability and tolerance of the immune environment.<sup>13, 31</sup> T<sub>reg</sub> cells prevent the overactivation of the immune system in inflammatory diseases.<sup>32</sup> Foxp3-positive T cells are typical anti-inflammatory cells that control and limit antigen-specific immune responses and immune tolerance.<sup>33, 34</sup> A previous study reported staining for Foxp3 (a T<sub>reg</sub> marker) in the striatal and cortical regions of the brain after ischemia and reperfusion in an MCAO-induced stroke model.<sup>35</sup> In our study, this protein was observed using LA-ICP MSI technology, which can evaluate the expression of several different proteins in a single test. We found for the first time that NBP significantly increases the content of Foxp3 in the ischemic area in an animal

stroke model. Additionally, NBP can play an anti-inflammatory and neuroprotective role by maintaining the function of Foxp3-positive T cells.

The most well-recognized mechanisms of action of NBP are improvements in the microcirculation, the promotion of angiogenesis, and increased cerebral blood flow in the ischemic area. Using LA-ICP MSI, we also found that NBP can increase the distribution of Ki-67 and pCREB in the ischemic cortex and striatum. Ki-67 is a nuclear protein involved in cell proliferation and can indicate vessel density.<sup>36</sup> Our study first explored the level of Ki-67 after NBP administration in an animal stroke model. The increase in the Ki-67 level in the ischemic area induced by NBP illustrated that NBP can improve angiogenesis in the ischemic region of the pMCAO model. NBP treatment also promotes the expression of vascular endothelial growth factor and angiopoietin-1 and induces angiogenesis.<sup>37</sup> Li et al. found that the Ang-1/Ang-2/Tie-2 signaling axis is altered in the cortex of chronic cerebral hypoperfusion rats and that NBP treatment can regulate this angiopoietin/Tie signaling axis in a timely manner to promote neovascularization in early stages.<sup>38</sup>

Cyclic-AMP response element-binding protein (CREB) is a protein that regulates gene transcription and is involved in synaptic plasticity, memory, and cognition.<sup>39</sup> The activation of the CREB pathway promotes nerve regeneration after cerebral ischemia-reperfusion in rats.<sup>40</sup> Liu B et al found Gadd45b-RNAi significantly decreased the expression levels of both BDNF and cAMP/PKA/phosphorylated cAMP response element-binding protein (pCREB) pathway and promoted ROCK expression. They conclude that Gadd45b stimulates recovery after stroke by enhancing axonal plasticity required for brain repair.<sup>41</sup> LA-ICP MSI showed that NBP can increase the level of phosphorylated CREB (pCREB) in the ischemic cortex and striatum, which is consistent with the results of Yang et al., indicating that NBP can improve nerve regeneration in the pMCAO model.<sup>42</sup> Nevertheless, how NBP exerts nerve regeneration and protects cognitive function deserves further research.

We demonstrated that NBP can reduce inflammatory damage, maintain immune tolerance, improve vascular density, and promote nerve cell regeneration through mechanisms that are shown in Fig. 5.

## Conclusion

NBP improves neurobehavior, reduces the area of brain damage, alleviates inflammation, and promotes nerve regeneration and angiogenesis in a rat model of pMCAO-induced cerebral ischemia.

We found that NBP can reverse abnormal changes in various phospholipid molecules, Foxp3, Ki-67 and pCREB, in the brain tissues of pMCAO rat models. The potential anti-inflammatory mechanism of NBP involves the inhibition of NLRP3 inflammasome, Caspase-1 and IL-1 $\beta$  overexpression to further alleviate the inflammatory reaction and improve brain tissue damage. Nevertheless, how NBP promotes nerve regeneration and angiogenesis requires further study.

## Abbreviations

<b>Abbreviations</b>	<b>Unabbreviations</b>
NBP	DI-3-n-butylphthalide
UK	Urinary kallidinogenase
ED	Edaravone
pMCAO	Permanent middle cerebral artery occlusion
MALDI-TOF MSI	Matrix-assisted laser desorption ionization time-of-flight mass spectrometry imaging
LA-ICP MSI	Laser ablation-inductively coupled plasma mass spectrometry imaging
mNSS	Modified neurological severity score
T <sub>reg</sub>	Regulatory T
FFPE	Formalin-fixed and paraffin-embedded

## **Declarations**

### **Ethics approval and consent to participate**

All operations were performed in accordance with the requirements of the Peking University Animal Experiment Ethics Committee (approval number: LA2016159) and the US Academy of Sciences Laboratory Animal Care and Use Guide.

### **Consent for publication**

Not applicable.

### **Availability of data and materials**

All data generated or analysed during this study are included in this published article and its supplementary information files.

### **Competing interests**

The authors declared no potential conflicts of interest with respect to the research, authorship, and/or publication of this article.

### **Funding**

This work was supported by Science and Technology Major Projects: Significant New-Drugs Creation (Grant no. 2018ZX09711001-009-006).

## Authors' contributions

Xi Liu: development of methodology, analysis and interpretation of data, writing of the manuscript.

Runzhe Liu: development of methodology, analysis and interpretation of data, writing of the manuscript.

Dongxu Fu: data analysis of LA-ICP MSI.

Hao Wu: interpretation of data.

Xin Zhao: review of the manuscript.

Yi Sun: review of the manuscript.

Meng Wang: support of LA-ICP MSI.

Xiaoping Pu: conception and design, revision of the manuscript.

## Acknowledgements

Not applicable.

## References

1. Wu S, Wu B, Liu M, et al. Stroke in China: advances and challenges in epidemiology, prevention, and management. *Lancet Neurol.* 2019;18:394–405.
2. Gelderblom M, Leyboldt F, Steinbach K, et al. Temporal and spatial dynamics of cerebral immune cell accumulation in stroke. *Stroke.* 2009;40:1849–57.
3. Petrovic-Djergovic D, Goonewardena SN, Pinsky DJ. Inflammatory Disequilibrium in Stroke. *Circ Res.* 2016;119:142–58.
4. Allan SM, Parker LC, Collins B, Davies R, Luheshi GN, Rothwell NJ. Cortical cell death induced by IL-1 is mediated via actions in the hypothalamus of the rat. *Proc Natl Acad Sci U S A.* 2000;97:5580–5.
5. Offner H, Subramanian S, Parker SM, et al. Splenic atrophy in experimental stroke is accompanied by increased regulatory T cells and circulating macrophages. *Journal of immunology (Baltimore, Md. 1950).* 2006; 176: 6523-31.
6. Bonaventura A, Liberale L, Vecchie A, et al. Update on Inflammatory Biomarkers and Treatments in Ischemic Stroke. *International journal of molecular sciences.* 2016; 17.
7. Zhang T, Jia W, Sun X. 3-n-Butylphthalide (NBP) reduces apoptosis and enhances vascular endothelial growth factor (VEGF) up-regulation in diabetic rats. *Neurological research.* 2010;32:390–6.
8. Abdoulaye IA, Guo YJ. A Review of Recent Advances in Neuroprotective Potential of 3-N-Butylphthalide and Its Derivatives. *BioMed research international.* 2016; 2016: 5012341.

9. Yang M, Dang R, Xu P, et al. DI-3-n-Butylphthalide improves lipopolysaccharide-induced depressive-like behavior in rats: involvement of Nrf2 and NF- $\kappa$ B pathways. *Psychopharmacology*. 2018;235:2573–85.
10. Geng C, Guo Y, Qiao Y, et al. UPLC-Q-TOF-MS profiling of the hippocampus reveals metabolite biomarkers for the impact of DI-3-n-butylphthalide on the lipopolysaccharide-induced rat model of depression. *Neuropsychiatr Dis Treat*. 2019;15:1939.
11. Liu RZ, Fan CX, Zhang ZL, et al. Effects of DI-3-n-butylphthalide on Cerebral Ischemia Infarction in Rat Model by Mass Spectrometry Imaging. *International journal of molecular sciences*. 2017; 18.
12. Ito M, Komai K, Mise-Omata S, et al. Brain regulatory T cells suppress astrogliosis and potentiate neurological recovery. *Nature*. 2019;565:246–50.
13. Sakaguchi S, Miyara M, Costantino CM, Hafler DA. FOXP3 + regulatory T cells in the human immune system. *Nat Rev Immunol*. 2010;10:490–500.
14. Fontenot JD, Gavin MA, Rudensky AY. Foxp3 programs the development and function of CD4 + CD25 + regulatory T cells. *Nat Immunol*. 2003;4:330–6.
15. Huang R, Xia M, Sakamuru S, et al. Modelling the Tox21 10 K chemical profiles for in vivo toxicity prediction and mechanism characterization. *Nature communications*. 2016;7:10425.
16. Stubbe T, Ebner F, Richter D, et al. Regulatory T cells accumulate and proliferate in the ischemic hemisphere for up to 30 days after MCAO. *Journal of cerebral blood flow metabolism: official journal of the International Society of Cerebral Blood Flow Metabolism*. 2013;33:37–47.
17. Chen J, Sanberg PR, Li Y, et al. Intravenous administration of human umbilical cord blood reduces behavioral deficits after stroke in rats. *Stroke*. 2001;32:2682–8.
18. Liu H, Chen R, Wang J, et al. 1,5-Diaminonaphthalene hydrochloride assisted laser desorption/ionization mass spectrometry imaging of small molecules in tissues following focal cerebral ischemia. *Analytical chemistry*. 2014;86:10114–21.
19. Toghi Eshghi S, Yang S, Wang X, Shah P, Li X, Zhang H. Imaging of N-linked glycans from formalin-fixed paraffin-embedded tissue sections using MALDI mass spectrometry. *ACS chemical biology*. 2014;9:2149–56.
20. Paton C, Hellstrom J, Paul B, Woodhead J, Hergt J. Iolite: Freeware for the Visualisation and Processing of Mass Spectrometric Data. *J Anal At Spectrom VL - IS* . 2011; online.
21. dos Santos G, Rogel MR, Baker MA, et al. Vimentin regulates activation of the NLRP3 inflammasome. *Nature communications*. 2015;6:6574.
22. Longa EZ, Weinstein PR, Carlson S, Cummins R. Reversible middle cerebral artery occlusion without craniectomy in rats. *Stroke*. 1989;20:84–91.
23. Qin C, Zhou P, Wang L, et al. DI-3-N-butylphthalide attenuates ischemic reperfusion injury by improving the function of cerebral artery and circulation. *Journal of cerebral blood flow metabolism: official journal of the International Society of Cerebral Blood Flow Metabolism*. 2019;39:2011–21.

24. Hare D, Austin C, Doble P. Quantification strategies for elemental imaging of biological samples using laser ablation-inductively coupled plasma-mass spectrometry. *Analyst*. 2012;137:1527–37.
25. Lefcoski S, Kew K, Reece S, et al. Anatomical-Molecular Distribution of EphrinA1 in Infarcted Mouse Heart Using MALDI Mass Spectrometry Imaging. *J Am Soc Mass Spectrom*. 2018;29:527–34.
26. Huang L, Chen C, Zhang X, et al. Neuroprotective Effect of Curcumin Against Cerebral Ischemia-Reperfusion Via Mediating Autophagy and Inflammation. *Journal of molecular neuroscience: MN*. 2018;64:129–39.
27. Abulafia DP, de Rivero Vaccari JP, Lozano JD, Lotocki G, Keane RW, Dietrich WD. Inhibition of the inflammasome complex reduces the inflammatory response after thromboembolic stroke in mice. *J Cereb Blood Flow Metab*. 2009;29:534–44.
28. Deroide N, Li X, Lerouet D, et al. MFG8 inhibits inflammasome-induced IL-1 $\beta$  production and limits postischemic cerebral injury. *J Clin Invest*. 2013;123:1176–81.
29. Dong X, Gao J, Zhang CY, Hayworth C, Frank M, Wang Z. Neutrophil Membrane-Derived Nanovesicles Alleviate Inflammation To Protect Mouse Brain Injury from Ischemic Stroke. *ACS Nano*. 2019;13:1272–83.
30. Yang CS, Guo A, Li Y, Shi K, Shi FD, Li M. DI-3-n-butylphthalide Reduces Neurovascular Inflammation and Ischemic Brain Injury in Mice. *Aging disease*. 2019;10:964–76.
31. Meng X, Yang J, Dong M, et al. Regulatory T cells in cardiovascular diseases. *Nat Rev Cardiol*. 2016;13:167–79.
32. McGeachy MJ, Stephens LA, Anderton SM. Natural recovery and protection from autoimmune encephalomyelitis: contribution of CD4 + CD25 + regulatory cells within the central nervous system. *J Immunol*. 2005;175:3025–32.
33. Zozulya AL, Wiendl H. The role of regulatory T cells in multiple sclerosis. *Nature clinical practice Neurology*. 2008;4:384–98.
34. Lu L, Barbi J, Pan F. The regulation of immune tolerance by FOXP3. *Nature reviews Immunology*. 2017;17:703–17.
35. Elango C, Devaraj SN. Immunomodulatory effect of Hawthorn extract in an experimental stroke model. *J Neuroinflamm*. 2010;7:97.
36. Jain A, Kratimenos P, Koutroulis I, Jain A, Buddhavarapu A, Ara J. Effect of Intranasally Delivered rh-VEGF165 on Angiogenesis Following Cerebral Hypoxia-Ischemia in the Cerebral Cortex of Newborn Piglets. *International journal of molecular sciences*. 2017; 18.
37. Zhou PT, Wang LP, Qu MJ, et al. DI-3-N-butylphthalide promotes angiogenesis and upregulates sonic hedgehog expression after cerebral ischemia in rats. *CNS Neurosci Ther*. 2019;25:748–58.
38. Li W, Wei D, Xie X, Liang J, Song K, Huang L. DI-3-n-Butylphthalide regulates the Ang-1/Ang-2/Tie-2 signaling axis to promote neovascularization in chronic cerebral hypoperfusion. *Biomedicine pharmacotherapy = Biomedecine pharmacotherapie*. 2019;113:108757.

39. Ashabi G, Sarkaki A, Khodagholi F, et al. Subchronic metformin pretreatment enhances novel object recognition memory task in forebrain ischemia: behavioural, molecular, and electrophysiological studies. *Can J Physiol Pharmacol*. 2017;95:388–95.
40. Zhu DY, Lau L, Liu SH, Wei JS, Lu YM. Activation of cAMP-response-element-binding protein (CREB) after focal cerebral ischemia stimulates neurogenesis in the adult dentate gyrus. *Proc Natl Acad Sci USA*. 2004;101:9453–7.
41. Liu B, Li LL, Tan XD, et al. Gadd45b Mediates Axonal Plasticity and Subsequent Functional Recovery After Experimental Stroke in Rats. *Mol Neurobiol*. 2015;52:1245–56.
42. Yang LC, Li J, Xu SF, et al. L-3-n-butylphthalide Promotes Neurogenesis and Neuroplasticity in Cerebral Ischemic Rats. *CNS Neurosci Ther*. 2015;21:733–41.

## Figures

**Figure 1**

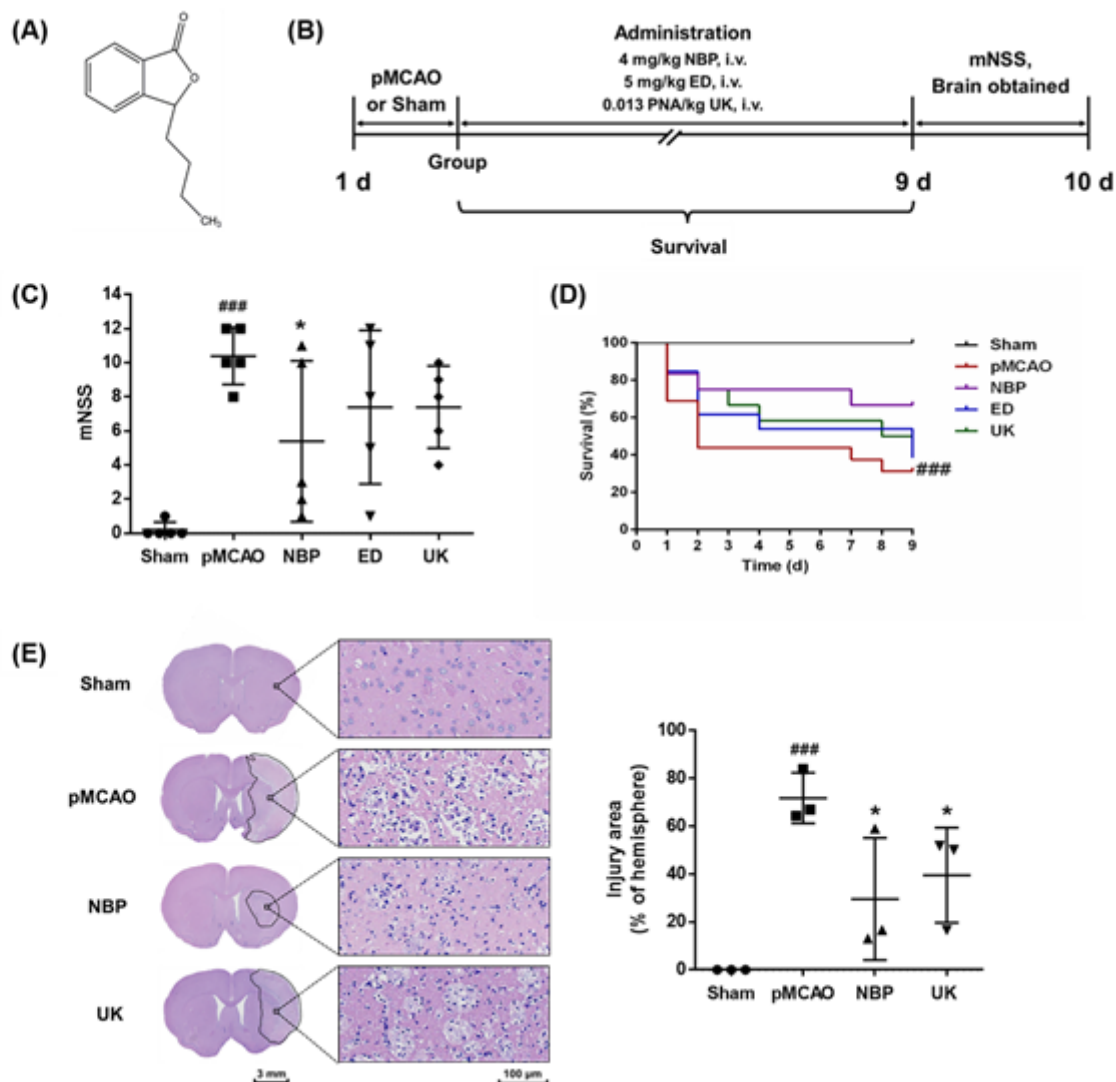


**Figure 1**

NBP treatment attenuated brain injury after pMCAO. (A) Structure of I-NBP. Racemic NBP was utilized in this study. (B) Experimental schematic. The pMCAO model was established, grouped, and then, drug administration was administered via the tail vein for 9 days. (C) The modified neurological severity scores (mNSS) of various groups. The data are presented as the mean  $\pm$  SD,  $n = 5$ . (D) The survival function of groups. (E) Representative images of brain morphology and statistical analysis of injury area, as revealed by HE staining. The striatum on the lesioned side was scanned at 200 $\times$  and is shown on the right. Scale bar = 3 mm for the full coronal section. Scale bar = 100  $\mu$ m for microscopic observation. The injury area was delineated by Motic DSAssistant Lite and analyzed by ImageJ. Sham: sham surgery group; pMCAO: permanent middle cerebral artery occlusion group; NBP: dl-3-n-butylphthalide-treated group; ED: edaravone-treated group; UK: urinary kallidinogenase-treated group. ###  $P < 0.001$  vs. the sham group, \*  $P < 0.05$  vs. the pMCAO group.

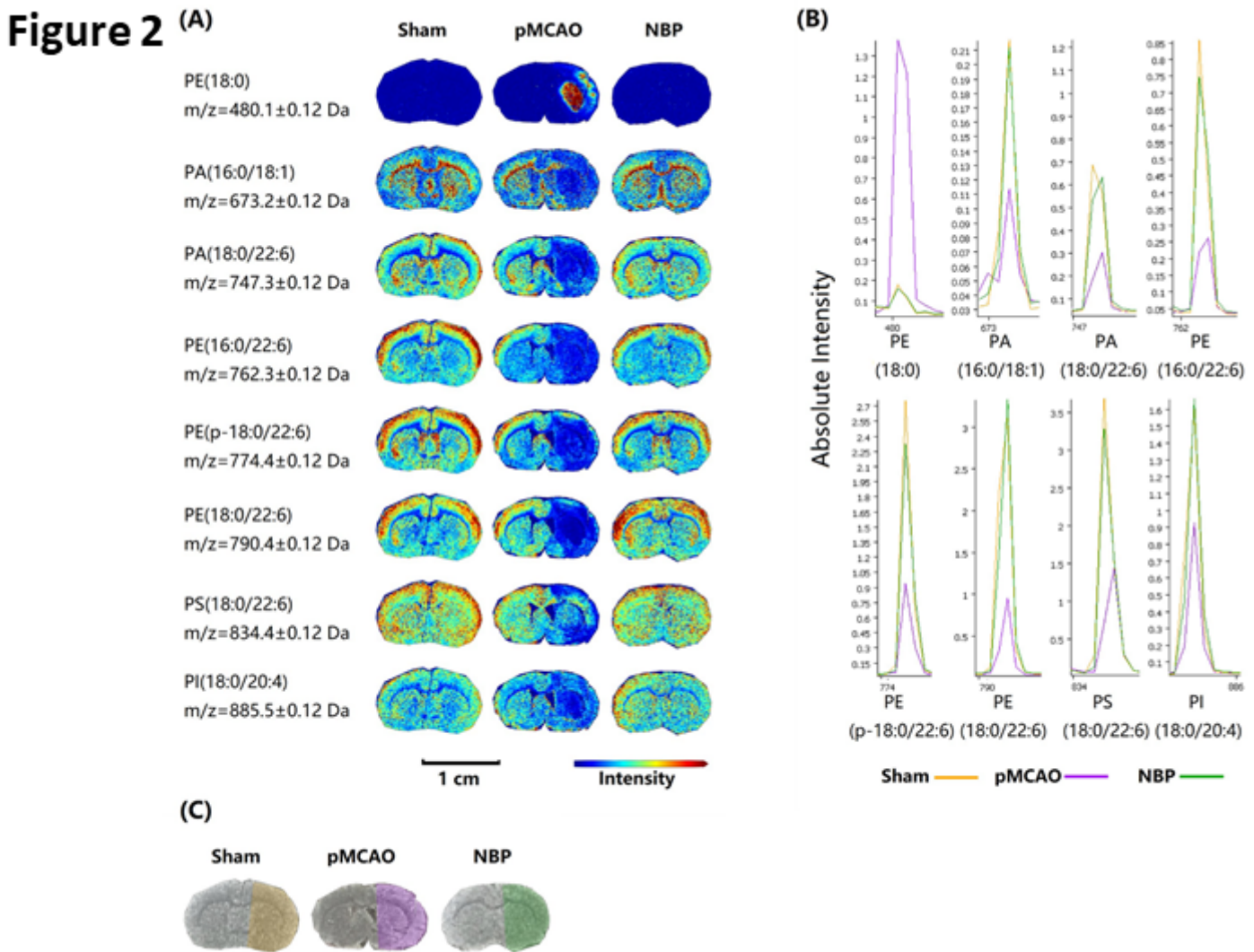


**Figure 2**

Change in phospholipids in the brains of rats with pMCAO. (A) In situ MALDI-TOF MSI of PE (18:0), PA (16:0/18:1), PA (18:0/22:6), PE (16:0/22:6), PE (p-18:0/22:6), PE (18:0/22:6), PS (18:0/22:6) and PI (18:0/20:4). The spatial resolution was set to 100  $\mu$ m. Scale bar=1 cm. (B)(C) The absolute intensity of the phospholipids mentioned above. The regions of interest (ROIs) are shown, and the peak mass spectra

intensities are displayed in the same color as the corresponding ROI. Sham: sham surgery group; pMCAO: permanent middle cerebral artery occlusion group; NBP: dl-3-n-butylphthalide-treated group.

### Figure 3

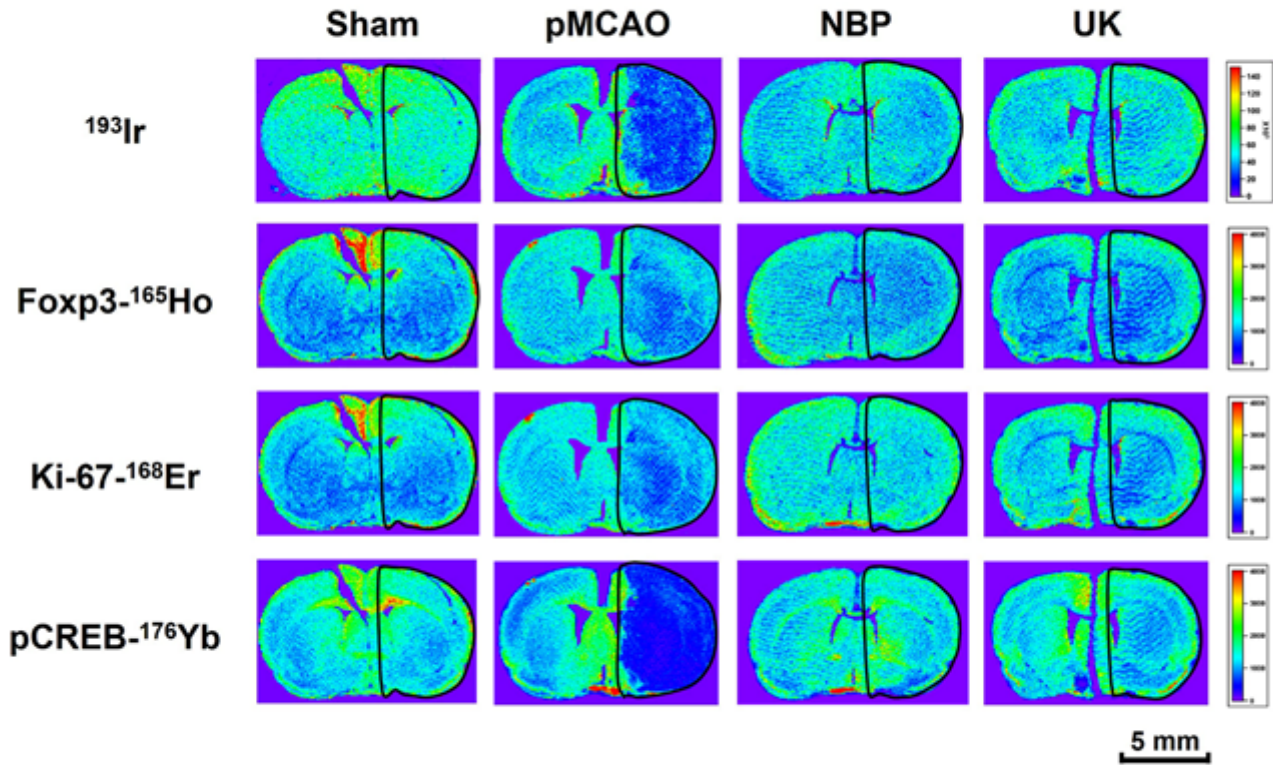


### Figure 3

Representative LA-ICP MS images of the intercalator  $^{193}\text{Ir}$ , Fxp3, Ki-67, and pCREB in the brain tissues of rats with pMCAO. For all tissues,  $^{193}\text{Ir}$  and three metal-labeled proteins were measured simultaneously at a resolution of  $110\ \mu\text{m}$ . Scale bars = 5 mm. Sham: sham surgery group; pMCAO: permanent middle cerebral artery occlusion group; NBP: dl-3-n-butylphthalide-treated group; UK: urinary kallidinogenase-treated group.

**Figure 4**

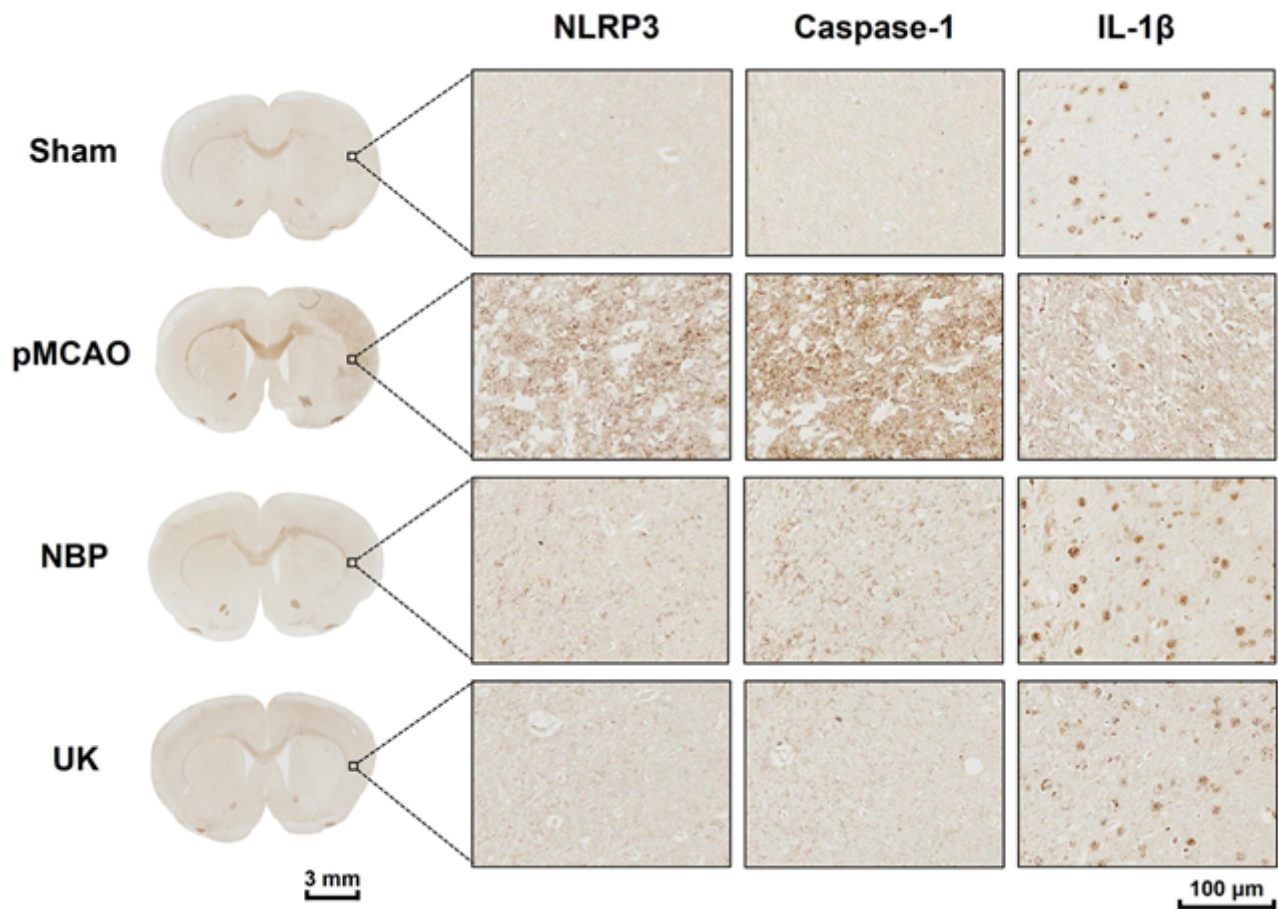


**Figure 4**

Expression of NLRP3, Caspase-1 and IL-1 $\beta$  in the right striatum of brain tissues of rats from each group. The striatum on the lesioned side was scanned at 200 $\times$  and is shown on the right. Scale bar = 3 mm for the full coronal section. Scale bar = 100  $\mu$ m for microscopic observation. Sham: sham surgery group; pMCAO: permanent middle cerebral artery occlusion group; NBP: dl-3-n-butylphthalide-treated group; UK: urinary kallidinogenase-treated group. n = 3.

**Figure 5**

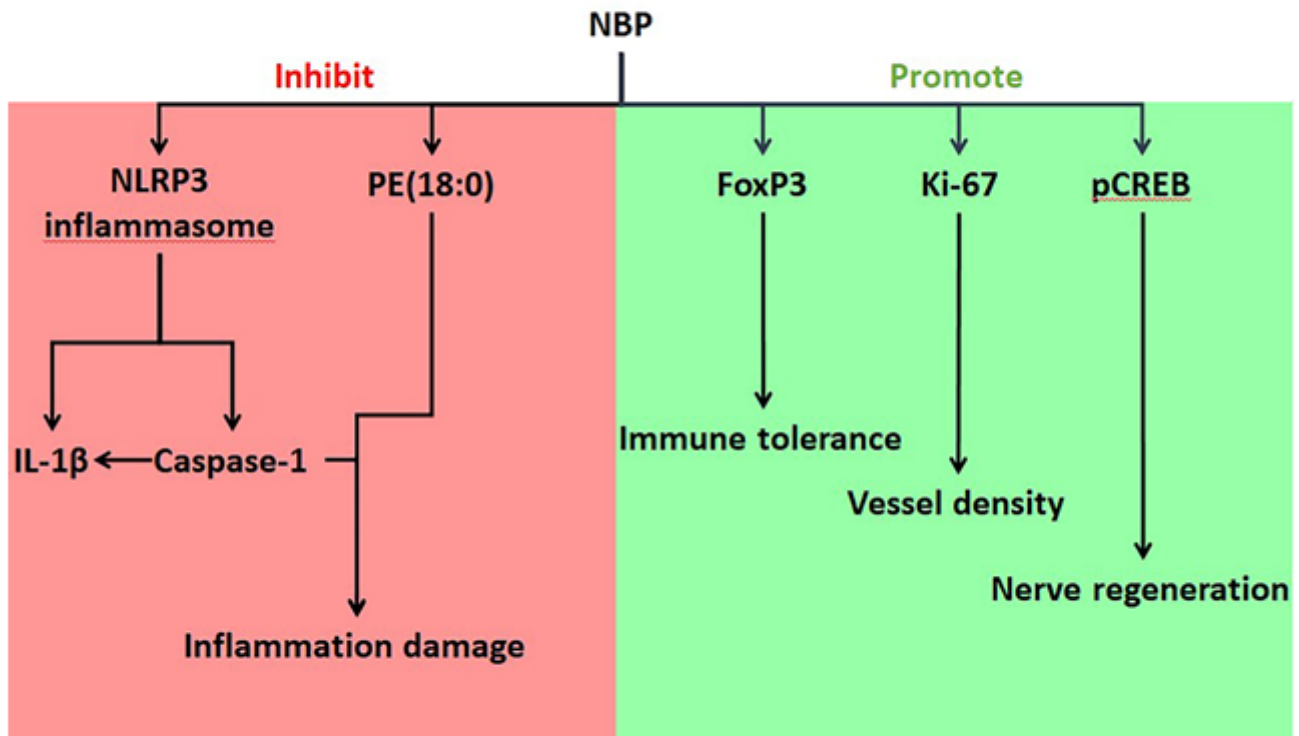


**Figure 5**

Effects of NBP on ischemic stroke in pMCAO rats and the associated mechanisms

## Supplementary Files

This is a list of supplementary files associated with this preprint. Click to download.

- [Supplementarymaterial.docx](#)